RSC Advances

ROYAL SOCIETY OF CHEMISTRY

www.rsc.org/advances

Continuous release of gentamicin from gold nanocarriers

by

Stefano Perni [1,2], Polina Prokopovich[1,2 *]

[1] School of Pharmacy and Pharmaceutical Sciences, Cardiff University, Cardiff, UK

[2] Center for Biomedical Engineering, Massachusetts Institute of Technology, Cambridge, USA

* Corresponding author:

Dr. Polina Prokopovich e-mail: prokopovichp@cardiff.ac.uk

School of Pharmacy and Pharmaceutical Sciences

Cardiff University

Redwood Building, King Edward VII Avenue

Cardiff, UK

CF10 3NB

Tel: +44 (0)29 208 75820 Fax: +44 (0)29 208 74149

Abstract

Antibiotics are still the most effective agents used to fight bacterial infections. Antibiotics are quickly metabolised or excreted from the human body, thus they need to be frequent administrated (few times a day) and their half life is usually an important factor in the therapeutic choice. In order to render the administration less frequent, antibiotic release from a carrier can be employed.

In this work we covalently bound gentamicin to gold nanoparticles capped with cysteine or glutathione as gold nanoparticles are biologically safe. The conjugates exhibited antimicrobial activity against both *S. aureus* and MRSA at concentrations as low as 0.1 mg NP/ml consistent with an antibiotic load of 1-2 % w/w as determined through TGA. No antimicrobial activity was exhibited by the unconjugated nanoparticles. The release of gentamicin from the conjugates was monitor in buffer solutions at pH = 7 and the antibiotic concentration continued increasing over two days.

This work demonstrates that gold nanoparticles can be employed as antibiotic carriers providing a continious release of antibiotic over few days. Glutathione appeared a better coupling agent than cysteine allowing higher load of gentamicin resulting in lower inhibitory conjugate concentrations.

Keywords: gold conjugates, gentamicin, *S. aureus*, MRSA, drug release

Introduction

Microorganisms can be classified in two distinct categories: non-pathogenic and pathogenic. Cells belonging to the later are responsible for infections; however, microorganisms can induce infections in some host species but not in others, i.e. human pathogens may not be pathogenic to animals and via versa. Antibiotics are still the most effective agents used to fight bacterial infections; they can be classified depending on the drug molecules structure (penicillin, tetracycline, cephalosporin, glycopeptide...), mechanism of action (membrane synthesis, protein synthesis, DNA) or their spectrum of activity. Their administration to patients is generally through oral, topical or parental route 1; antibiotics are quickly metabolised and excreted from the human body; hence their concentration rapidly decreases after administration, this leads to the need for frequent administration and their half-life is usually an important factor in the therapeutic choice. In order to render the administration less frequent and to improve efficacy, antibiotic release from a carrier has been suggested as possible approach. 2-6

Gold nanoparticles have found numerous applications as drug delivery vehicles because of their stability and biological safety. 7-9 Their synthesis is generally performed through the reduction of Au^{3+} using inorganic agents or through biogenic approaches. Capping agents such as: tiopronin [10], glutathione [11] and L-cysteine [12] have also been employed exploiting the thiol affinity toward gold; moreover they provide stability to the particles and to allow further grafting of molecules to the gold carrier.

Stimuli responsive delivery systems have been developed to enhance the efficacy of drugs; [13] temperature and pH are examples of triggers used to enable drug release from a carrier. [14,15] pH responsive systems are generally based on three mechanisms, one is through a covalent bond between the carrier and the drug that is hydrolysed when required; for this porpoise an amide bond, stable at physiological pH and broken in acidic conditions, is used. [16-17] Alternatively, the drug is embedded in a polymer matrix that is dissolved at acidic pH. [18-21] Capsules coated with a sequence of oppositely charged polyelectrolytes containing the chosen drug can release it when the change of pH induces a variation of the charge in one of the two electrolytes thus reducing the electrostatic attraction. [22-24]

In this work, we synthesised gold nanoparticles capped with either glutathione or L-cysteine and covalently attached gentamicin to the capping agent; after characterising the physico-chemical properties of the conjugates, we determined the dose-response antimicrobial activity against *Staphylococcus aureus* and Methicillin resistant *S. aureus* of the conjugates along with the kinetic of antibiotic release.

Materials and Methods

Chemicals

$HAuCl_4 \bullet 3H_2O$ (99.99%), glutathione (99%), L-cysteine, hydrazine (80%), gentamicin (GS), (N-morpholino) ethanesulfonic acid (MES) buffer, 1-[3-(dimethylamino)-propyl]-3-ethylcarbodiimide hydrochloride (EDC), N-hydroxysulfo-succinimide sodium salt (sulfo-NHS) and *o*-phthaldialdehyde reagent solution (OPA) were purchased from Sigma, UK. Methanol and *iso*-propanol were purchased from Fisher, UK.

Buffers were prepared according to standard laboratory procedures. All other chemicals were reagent grade, stored according to manufacturer's guidelines and used as received.

Conjugates preparation

Typically, gold nanoparticles were synthesised from 60 ml of an acidified aqueous solution (acetic acid:dH_2O 1:5) of $HAuCl_4$ (17 mM) containing glutathione or L-cysteine (8 mM) as capping agent adding 0.2 ml of hydrazine 80% drop wise under vigorous mixing. The nanoparticles were separated after 1 hour at room temperature adding 50 ml of methanol and centrifuging for 10 min at 2455 g (Avanti J-25, Beckman-Coulter). The processed was repeated three time and the gold nanoparticles were allowed to dry on a glass watch for 24 hours.

Conjugates were prepared dispersing the 100 mg of Au nanoparticles in 50 ml MES buffer (50 mM, pH 6.5) in the presence of gentamicin (50 mg) along with sulfo-NHS (25 mg) and EDC (45 mg). After 24 h at room temperature under vigorous mixing, the conjugates were separated adding 25 ml of methanol and centrifuging for 10 min at 2455 g (Avanti J-25, Beckman-Coulter). The process was repeated three time and the gold nanoparticles were allowed to dry on a glass watch for 24 hours.

Conjugates characterisation

UV-vis spectra (400 - 700 nm, 1 nm resolution) of the conjugated dispersed in PBS (1 mg/ml) were recorded in 1 cm quartz cells with a U-3000 Hitachi, UV-vis spectrometer.

Infrared spectra (from 4000 to 500 cm^{-1}) of the samples were collected with Perkin Elmer Spectrum One with Ge/Ge UATR.

For transmission electron microscopy (TEM) characterization a 4 µl droplet of nanoparticles suspension was placed on a plain carbon-coated copper TEM grid and allowed to evaporate in air under ambient laboratory conditions for several hours. Bright field TEM images were obtained using a TEM (Philips CM12, FEI Ltd, UK) operating at 80kV fitted with an X-ray microanalysis detector (EM-400 Detecting Unit, EDAX UK) utilising EDAX's Genesis software. Typical magnification of the images was x 100 000. Images were recorded using a SIS MegaView III digital camera (SIS Analytical, Germany) and analyzed with the software ImageJ; the diameter of at least 150 particles for each synthetic condition was determined.

Thermogravimetric analysis (TGA) was performed using a Stanton Redcroft, STA-780 series TGA; data were recorded from 25 to 600 °C with a constant heating rate of 10 °C $minute^{-1}$.

Gentamicin release quantification

Conjugates were dispersed in citric acid – Na_2HPO_4 buffer pH = 7 (5 mg/ml) and incubated at 37 °C. At prefixed times samples were taken and the gentamicin in the buffer was quantified thorough fluorescence spectroscopy using o-phthaldialdehyde. 100 µl of buffer containing gentamicin were mixed with 100 µl of iso-propanol and 100 µl of OPA reagent solution (Sigma, UK); after 30 min at room temperature in the dark, 200 µl of the mixture were transferred in a black 96 wells plate and the fluorescence determined (excitation wavelength = 340 nm and emission wavelength = 450 nm) with a fluoroscan (FLUOROstar Optina, BMG labtech); standards of known gentamicin concentration were also analysed simultaneously. The tests were performed in duplicates on conjugates from three independent batches.

Antimicrobial testing

Staphylococcus aureus (NCIMB 9518) and Methicillin resistant *S. aureus* - MRSA (NCTC 12493) were stored at -80 °C. Brain Heart Infusion (BHI) Agar plates were streaked with the frozen cultures and cells were grown at 37 °C for. Stocks were then stored at -4 °C for no more than a week. Cell cultures were prepared inoculating 10 ml of fresh sterile BHI broth and incubating at 37 °C statically for 24 hours. Cells were diluted in fresh BHI broth to a final concentration of 10^4 CFU/ml and 150 µl of this suspension were poured in each well of a row of a 96 wells plate. Au-gentamicin conjugates were dispersed in sterile BHI broth at a concentration of 14 mg/ml and 150 µl were added to the first well of the 96 wells plate. From this, 150 µl were poured in the second well resulting in half concentration of Au conjugates; the process was repeated as far the penultimate well; the last well was filled with PBS and acted as control. The plates were then incubated at 37 °C for 24 hours and bacterial cells were counted through serial dilutions in sterile PBS and plating on BHI Agar (plates incubated 24 hours at 37°C). The tests were performed on three independent cultures on conjugates from three independent batches.

Results and discussion

The gold conjugates were prepared in a two step synthesis; in the first the Au capped nanoparticles were prepared and purified, the second step was the conjugation of gentamicin to the nanoparticles via condensation reaction (Figure 1) in the presence of EDC and NHS to activate the carboxyl group present on both capping agents. The nanoparticles were synthesised according to a modified Brust method [25-27] where the acid pH of the aqueous solution was required to achieve stable nanoparticles whilst the undesired by-products and unreacted starting compounds were removed through methanol washing as the gold nanoparticles are non soluble in such solvent as verified by NMR.

The suspension of gold capped nanoparticles in PBS exhibited maximum absorbance at 560 nm, whilst the glutathione capped nanoparticles had a maximum shifted at 550 nm (Figure 2); this was in accordance with the colour of the aqueous suspension being dark red (for glutathione capped) to purple (L-cysteine capped). The gold conjugates appeared rounded (Figure 3) regardless of the capping agent (data not shown); the diameter was 5.2 ± 1.1 nm and 7.8 ± 1.2 for glutathione and L-

cysteine capped nanoparticles respectively; in both cases the conjugation did not affect the gold core size of the nanoparticles as expected and also found in previous gold conjugates. [11] These two results are in agreement as larger nanoparticles exhibit absorbance peaks at progressively greater wavelength (from red to purple to dark violet).

FTIR (Figure 4 and Figure 5) revealed that the hydrogen-sulphur bond of the -SH group presented in both glutathione and L-cysteine (at ~2560 cm^{-1}) disappeared after the synthesis of the gold nanoparticles demonstrating the stabilisation conferred to the nanoparticles by the strong affinity of gold for sulphur. Other than the -SH band the spectra of the capped gold nanoparticles were remarkably similar to those of the pure capping agent; whilst the further binding of gentamicin to either glutathione or L-cysteine was not detectable through FTIR.

The organic fraction composition of the gold nanoparticles was determined through TGA (Figure 6a), both samples exhibited mass loss when the temperature increased above 150-200 °C corresponding to the loss of the organic fraction (capping agent and/or gentamicin), whilst the remaining fraction was the gold core of the conjugates the remained unaffected at temperatures as high as 600 °C; the profile of TGA analysis of the individual capping agents (Figure 6b) appeared similar to that of the gold nanoparticles but almost total thermal decomposition occurred; gentamicin was the most resistant to thermal degradation. The percentage of glutathione appeared less than L-cysteine, 17 % and 22 % w/w respectively. Additionally, the molar concentration of glutathione on the nanoparticles was also lower than cysteine; the molecular weight of cysteine is about a third of glutathione (307 vs. 121 g/mol) while the similar organic amount and size of the gold nanoparticles thus suggesting that steric interactions prevent glutathione coupling with gold. Similar amount of organic fraction were reported for glutathione capped gold nanoparticles despite different ratio between capping agent and Au^{3+} during nanoparticles preparation. The ratio between metal and thiol capping agent appeared to influence the amount of organic fraction for gold nanoparticles [10,11] as for silver. [28]

The amount of gentamicin bound to the conjugates was calculated as the difference between the metallic core of the capped nanoparticles and that of the conjugates. More gentamicin was present on glutathione capped (2.5 % w/w) than on L-cysteine capped gold nanoparticles (1.2 % w/w). This could be due to the two carboxyl groups exhibited by glutathione compared to the single carboxyl

group of cysteine. The simultaneous presence of amino and carboxyl groups in both capping agents could have resulted in inter-particles conjugation; however this was not observed in virtue of the high excess of gentamicin used. The molecular weight of the nanoparticles can be estimated to be around 1.2 10^6 g/mol (assuming a perfectly rounded particle made of metal gold (ρ = 19.3 g/cm^3) with a diameter of 6 nm), such the conjugation reaction employed ~ 0.080 μmol nanoparticles and ~ 100 μmol of gentamicin. Similar gold conjugates with tin-chlorin e6 (SnCe6) had comparable molecular weight and the analogous conjugation reaction (amide bond formation between glutathione and SnCe6) also in that case did not caused inter-particles bonding despite being carried out with lower molar ratio between reactant and particles than in this work.[11] *S. aureus* and MRSA were chosen in this work as main representatives of infectious agents; they are the main sources of infections related to i.e. intravenous catheters, post orthopaedic surgeries and community acquired infections. No antimicrobial activity was exhibited by the unconjugated nanoparticles at the highest concentration tested (3.5 mg NP/ml); this was expected as gold nanoparticles are known to be relatively inert against cells, nevertheless this was essential to prove the antimicrobial activity was due to only the antibiotic released from the nanocarriers.

The conjugates exhibited antimicrobial activity against *S. aureus* and MRSA (Figure 7 and Figure 8). When glutathione was employed, the MIC was 220 μg NP/ml irrespectively of the bacteria species tested. On the other hand, when cysteine was employed as capping agent, the MIC was 440 μg NP/ml for MRSA (Figure 7) and 880 μg NP/ml for *S. aureus* (Figure 8). For both bacterial species the MIC corresponded to the MBC.

Gentamicin was released from the glutathione capped Au conjugates for at least two days; however, when L-cysteine was used the released was completed after 24 hours (Figure 9). Furthermore, the overall amount of antibiotic released was greater for glutathione capped conjugates than L-cysteine. From the known amount of gentamicin conjugated to the gold nanoparticles in both cases, it is estimated that about 25% of the gentamicin bound was released after 48 hours when glutathione was used, whilst only about 10% was released from L-cysteine capped nanoparticles after the same time.

The MIC for pure gentamicin was 4 μg/ml for MRSA and less than 2 μg/ml for *S. aureus* (data not shown); therefore, the higher resistance of *S. aureus* to the conjugates is not related to the antibiotic used but is connected to interference of cells growth with the antibiotic release from the carrier, possibly through pH changes of the media. Moreover, the higher activity of the glutathione capped conjugates is related to the higher amount of gentamicin released from these nanocarriers.

The possibility of triggering the release using some environmental factor change (stimuli responsive system) has been suggested as an option to improve the efficacy of antibiotics. The approach would rely on the shift in pH from physiological to acidic when *Staphylococcus* infections develop; [24] these infections are common in patients after undergoing orthopaedic surgery. [1,29] In this way, antibiotics would remain unused when not required prolonging the time span of effectiveness of materials containing this drug delivery system; this proposition seems particularly suited to antibiotic laden bone cements as the commercial formulation (were antibiotic are simply mixed with the cement) generally stop releasing antibiotic after a few months, [2,30,31] whilst infection offset can occur even after years from implantation. [29] Irrespectively of the pH-response mechanism employed (bond breakable at acidic pH between carrier or polymer matrix dissolution), such approach would only respond to an infection already significantly developed, in virtue of the pH shift needed to trigger the release; it is very unlikely to provide an effective prevention approach. The main consequence of the need for infections to develop first before they could be treated is the inability of antibiotics to inactivate virulence factors already released in the tissue surrounding the pathogen cells. [32] Such compounds are produced by the bacteria during growth and are responsible for the damages caused by the infectious agent; for example *S. aureus* produces more than 40 virulence factors, [33] some of them are V8 protease, alpha-haemolysin causing lysis of red blood cells [33] and sphingomyelinase that are known to kill proliferating T lymphocytes, suggesting a role for this toxin in evasion of the host immune response. [34] Because of this, the perceived benefit of being able to retain antimicrobial activity would be counterbalanced by the greater damages and discomfort caused by infections when a pH responsive system is used.

Another major drawback of this technology would be the narrow spectrum of activity, narrower than the free antibiotic, as many infections, of significant incidence, do not result in pH changes, for

example *E. coli*. Hence, in such circumstances, the antibiotic would remain bound and the infection would need to be treated with a separate administration of antimicrobial drugs. The system developed here is capable of releasing antibiotic also at physiological pH, therefore would be able to retain the spectrum of activity of the original antibiotic, but the persistence release from the carrier would reduce the frequency/number of administrations, positively impacting on nurses time and patient compliance because simpler treatment protocols (i.e. few administrations) are more likely to be adhered than more complex ones. This impacts positively on the fight against the rise of antibiotic resistance among bacteria as the inappropriate use of antibiotics is a major cause in resistance rise and spread.

Conclusion

This work demonstrates that gentamicin can be conjugated to gold nanoparticles and that these can be employed as antibiotic carrier providing a continuous release of antibiotic over few days; hence they could constitute a delivery systems capable of reducing the number of administrations and, in turn, the direct cost associated and the indirect resulting from non compliance. The unconjugated gold nanoparticles do not exhibit any antimicrobial activity. Glutathione appeared a better capping agent than cysteine allowing higher load of gentamicin resulting in lower minimum inhibitory concentrations of the conjugate against both MRSA and *S. aureus*.

Acknowledgments

The authors would like to thank Arthritis Research UK (ARUK:18461) for providing financial support to this project.

References

1. Meehan J., Jamali A.A., Nguyen H. Prophylactic antibiotics in hip and knee arthroplasty. *J Bone Joint Surg Am.* 2009;91(10):2480-2490.

2. Shen S.C., Ng W.K., Shi Z., Chia L., Neoh K.G., Tan R.B.H. Mesoporous silica nanoparticle-functionalized poly(methylmethacrylate)-based bone cement for effective antibiotics delivery. *J Mater Sci: Mater Med* 2011;22:2283-2292

3. Honary, S., Ebrahimi, P., Hadianamrei, R. Optimization of particle size and encapsulation efficiency of vancomycin nanoparticles by response surface methodology. *Pharmaceutical Development And Technology* 2014 ;19(8) :987-998

4. Pourjavadi, A., Tehrani, Z.M. Mesoporous Silica Nanoparticles (MCM-41) Coated PEGylated Chitosan as a pH-Responsive Nanocarrier for Triggered Release of Erythromycin. *Int. J. Polymeric Materials And Polymeric Biomaterials* 2014;63(13):692-697

5. Lan Y., Li W., Jiao Y., Guo R., Zhang Y., Xue W., Zhang Y. Therapeutic efficacy of antibiotic-loaded gelatin microsphere/silk fibroin scaffolds in infected full-thickness burns. *Acta Biomater*. 2014;10(7):3167-3176

6. Rivadeneira J., Di Virgilio A.L., Audisio M.C., Boccaccini, A.R., Gorustovich, A.A. Evaluation of antibacterial and cytotoxic effects of nano-sized bioactive glass/collagen composites releasing tetracycline hydrochloride. *Journal Of Applied Microbiology* 2014;116(6):1438-1446

7. Colleen A.M., Hamner K..L., Maye M.M., Dabrowiak J.C. Multifunctional DNA-Gold Nanoparticles for Targeted Doxorubicin Delivery. *Bioconjugate chemistry* 2014;25(7):1261-1271

8. Ding Y., Jiang Z., Saha K., Kim C.S., Kim S.T., Landis R.F., Rutello V.M. Gold Nanoparticles for Nucleic Acid Delivery. *Molecular Therapy* doi:10.1038/mt.2014.30

9. Pissuwan D, Niidome T, Cortie MB. The forthcoming applications of gold nanoparticles in drug and gene delivery systems. *J. Control Release* 2011; 149:65-71

10. J. Gil-Thomas, S. Tubby, I. P. Parkin, N. Narband, L. Dekker, S. P. Nair, M. Wilson, C. Street, Lethal Photosensitisation of *Staphylococcus aureus* Using a Toluidine Blue O–Tiopronin–Gold Nanoparticle Conjugate. *J. Mater. Chem.*, 2007;17:3739-3746

11. J. Gil-Thomas, L. Dekker, N. Narband, I. P. Parkin, S. P. Nair, C. Street, M. Wilson. Lethal photosensitisation of bacteria using a tin chlorin e6–glutathione–gold nanoparticle conjugate. *J. Mater. Chem.*, 2011;21:4189-4196
12. Majzik A, Fülöp L, Csapó E, Bogár F, Martinek T, Penke B, Bíró G, Dékány I. Functionalization of gold nanoparticles with amino acid, beta-amyloid peptides and fragment. *Colloids Surf B Biointerfaces.* 2010:81(1):235-241
13. Mura S., Nicolas J., Couvreur P. Stimuli-responsive nanocarriers for drug delivery. *Nature Materials* 2013; 12: 991-1003
14. Araujo, M., Viveiros, R., Correia, T.R., Correia, I.J., Bonifácio V.D.B., Casimiro, T., Aguiar-Ricardo A. Natural melanin: A potential pH-responsive drug release device. *International Journal Of Pharmaceutics* 2014; 469(1):140-145
15. Setareh A., Duroux L., Nielsen T.T., Larsen K.L. Preparation and characterization of a temperature-sensitive nonwoven poly(propylene) with increased affinity for guest molecules. *J. Appl. Polym. Sci.* 2014, 131, 40497
16. Pichavant L., Bourget ., Durrieu M.C., Heroguez V. Synthesis of pH-Sensitive Particles for Local Delivery of an Antibiotic via Dispersion ROMP. *Macromolecules* 2011; 44:7879-7887
17. Pichavant L., Amadord G., Jacqueline C., Brouillaud B., Héroguez V., Durrieu M.C. pH-controlled delivery of gentamicin sulfate from orthopedic devices preventing nosocomial infections. *Journal of Controlled Release* 2012;162:373-381
18. Zhang C., Zhu Y., Zhou C., Yuan W., Du J. Antibacterial vesicles by direct dissolution of a block copolymer in water. *Polym. Chem.*, 2013, 4, 255-259
19. Wang G.H., Liu S.J., Ueng S.W.N., Chan E.C. The release of cefazolin and gentamicin from biodegradable PLA/PGA beads. *International Journal of Pharmaceutics* 2004;273:203-212
20. Lynn D.M., Amiji M.M. Langer R. pH-Responsive Polymer Microspheres: Rapid Release of Encapsulated Material within the Range of Intracellular pH. *Angew. Chem. Int. Ed.* 2001;40(9):1707-1710
21. Xu Q., Czernuszka J.T. Controlled release of amoxicillin from hydroxyapatite-coated poly(lactic-co-glycolic acid) microspheres. *Journal of Controlled Release* 2008;127:146-153

22. F. Cuomo, F. Lopez, A. Ceglie, L. Maiuro, M. G. Miguel, B. Lindman. pH-responsive liposome-templated polyelectrolyte nanocapsules. *Soft Matter* 2012;8:4415-4420
23. D. Lundberg, A.M. Carnerup, J. Janiak, K. Schille, M. Miguel, B. Lindman. Size and morphology of assemblies formed by DNA and lysozyme in dilute aqueous mixtures. *Phys. Chem. Chem. Phys.* 2011;13:3082-3091
24. S. Pavlukhina, Y. Lu, A. Patimetha, M. Libera, S. Sukhishvili, Polymer multilayers with pH-triggered release of antibacterial agents, *Biomacromolecules* 2010;11(12):3448–3456
25. M. Brust, J. Fink, D. Bethell, D. J. Schiffrin and D. Kiely, *J. Chem. Soc., Chem. Commun*., 1995, 1655
26. M. Brust and C. J. Kiely, *Colloids Surf., A*, 2002, 202, 175
27. A. C. Templeton, W. P. Wuelfing and R. W. Murray, *Acc. Chem. Res*., 2000, 33, 27
28. P. Prokopovich, R. Leech, C.J. Carmalt, I.P. Parkin, S. Perni. A Novel Bone Cement Impregnated with Silver-tiopronin Nanoparticles: its Antimicrobial, Cytotoxic and Mechanical Properties. *Int. J. Nanomed.* 2013;8(1):2227-2237
29. JW Sperling, TK Kozak, AD Hanssen, RH Cofield: Infection after shoulder arthroplasty. *Clin Orthop Relat Res.* 2001;382:206-216
30. Penner M.J., Duncan C.E., Masri B.A. The In Vitro Elution Characteristics of Antibiotic-Loaded CMW and Palacos-R Bone Cements. *The Journal of Arthroplasty* 1999;14(2):209-214
31. van de Belt H., Neut D., Uges D.R., Schenk W., van Horn J.R., van der Mei H.C., Busscher H.J. Surface roughness, porosity and wettability of gentamicin-loaded bone cements and their antibiotic release. *Biomaterials* 2000;21(19):1981-1987
32. Tubby S, Wilson M, Nair SP. Inactivation of staphylococcal virulence factors using a light-activated antimicrobial agent. *BMC Microbiol.* 2009;9:211
33. Dinges MM, Orwin PM, Schlievert PM. Exotoxins of Staphylococcus aureus. *Clin Microbiol Rev.* 2000;13(1):16-34

331 34. Huseby M, Shi K, Brown CK, Digre J, Mengistu F, Seo KS, Bohach GA, Schlievert PM,
332 Ohlendorf DH, Earhart CA. Structure and biological activities of beta toxin from
333 Staphylococcus aureus. *J Bacteriol.* 2007; 189(23):8719-8726

Figure captions

Figure 1. Reaction scheme for Au gold nanoparticles capped with glutathione.

Figure 2. UV-vis spectra of Au nanoparticles capped with glutathione (solid line) and L-cysteine (dashed line).

Figure 3. Example of TEM image for gold nanoparticles capped with glutathione. Bar equivalent to 100 nm.

Figure 4. Infrared spectra of glutathione (solid line), gentamicin (dashed and dotted line), Au-glutathione conjugates (dotted line) and Au-glutathione-gentamicin (dashed line) from 4000 to 400 cm^{-1}.

Figure 5. Infrared spectra of L-cysteine (solid line), Au-L-cysteine conjugates (dotted line) and Au-L-cysteine-gentamicin (dashed line) from 4000 to 400 cm^{-1}.

Figure 6. Thermal Gravimetric Analysis (TGA) of Au conjugates (a) and pure compounds (b).

——— Au-glutathione ····· Au-glutathione-GS

- - - - - - Au-L-cysteine —··—·· Au-L-cysteine -GS

——— glutathione —··—·· L-cysteine - - - - - - GS

355 Figure 7. Antimicrobial activity of Au-glutathione (a) and Au-L-cysteine (b) against MRSA. Solid bar
356 conjugates conjugates with gentamicin and white bars conjugates without gentamicin. * represent
357 bacterial count below detection limit

358

359 Figure 8. Antimicrobial activity of Au-glutathione (a) and Au-L-cysteine (b) against *S. aureus*. Solid
360 bar conjugates conjugates with gentamicin and white bars conjugates without gentamicin.* represent
361 bacterial count below detection limit

362

363 Figure 9. Release of gentamicin from Au-glutathione (●) and Au-L-cysteine (○) over time in buffer
364 pH = 7

365

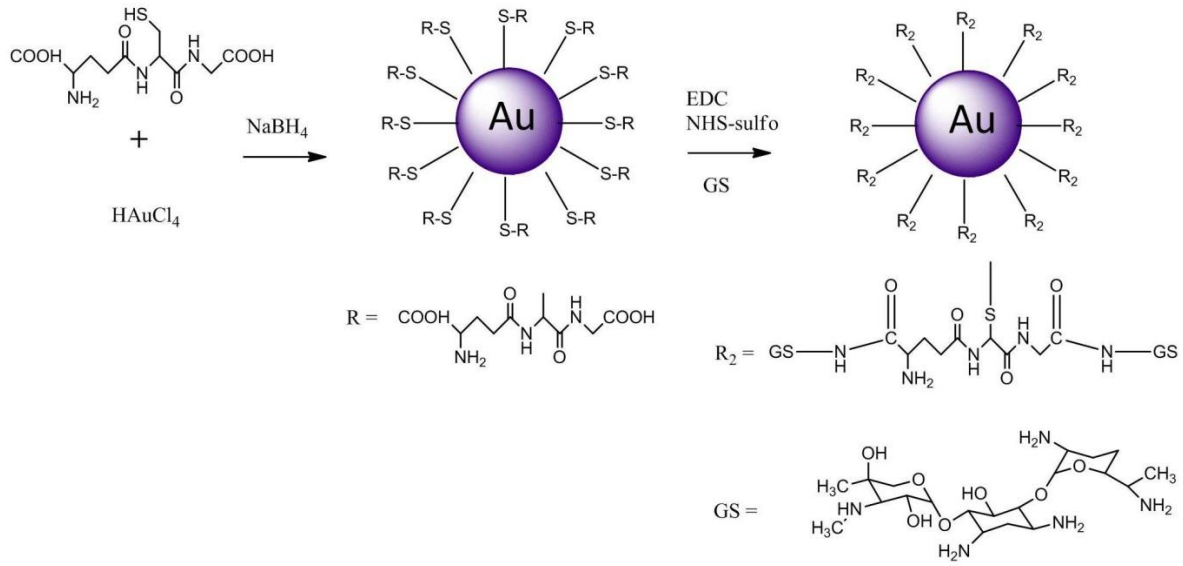

366

367 Figure 1

368

369

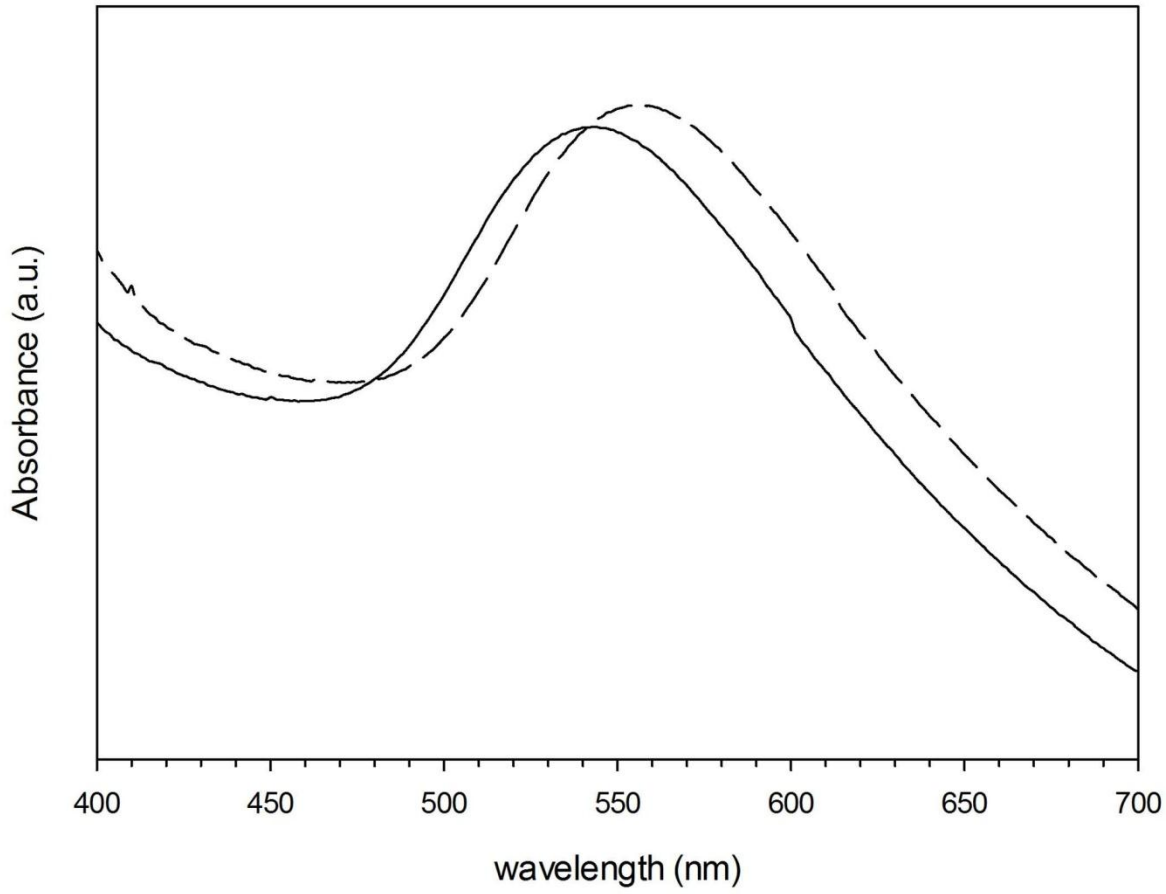

370

371 Figure 2

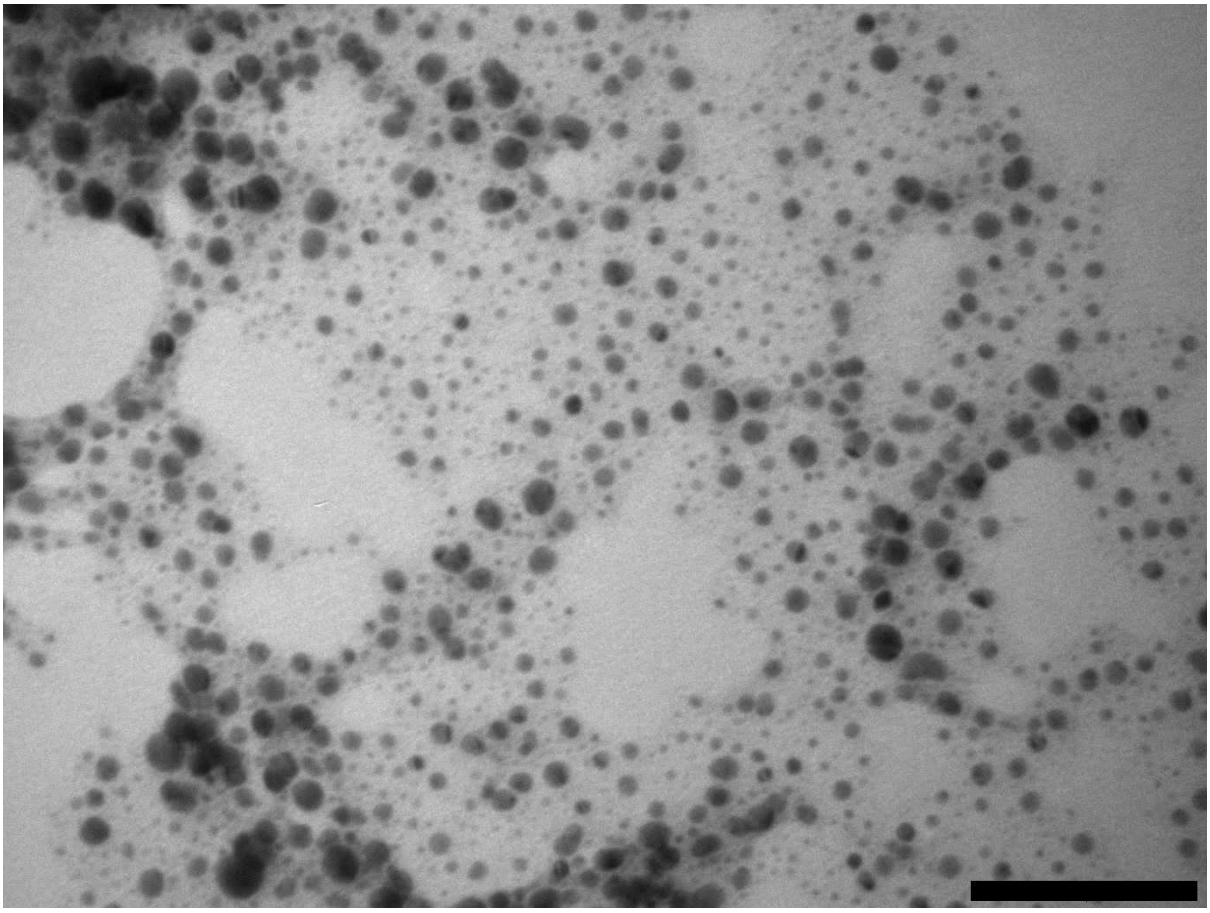

Figure 3

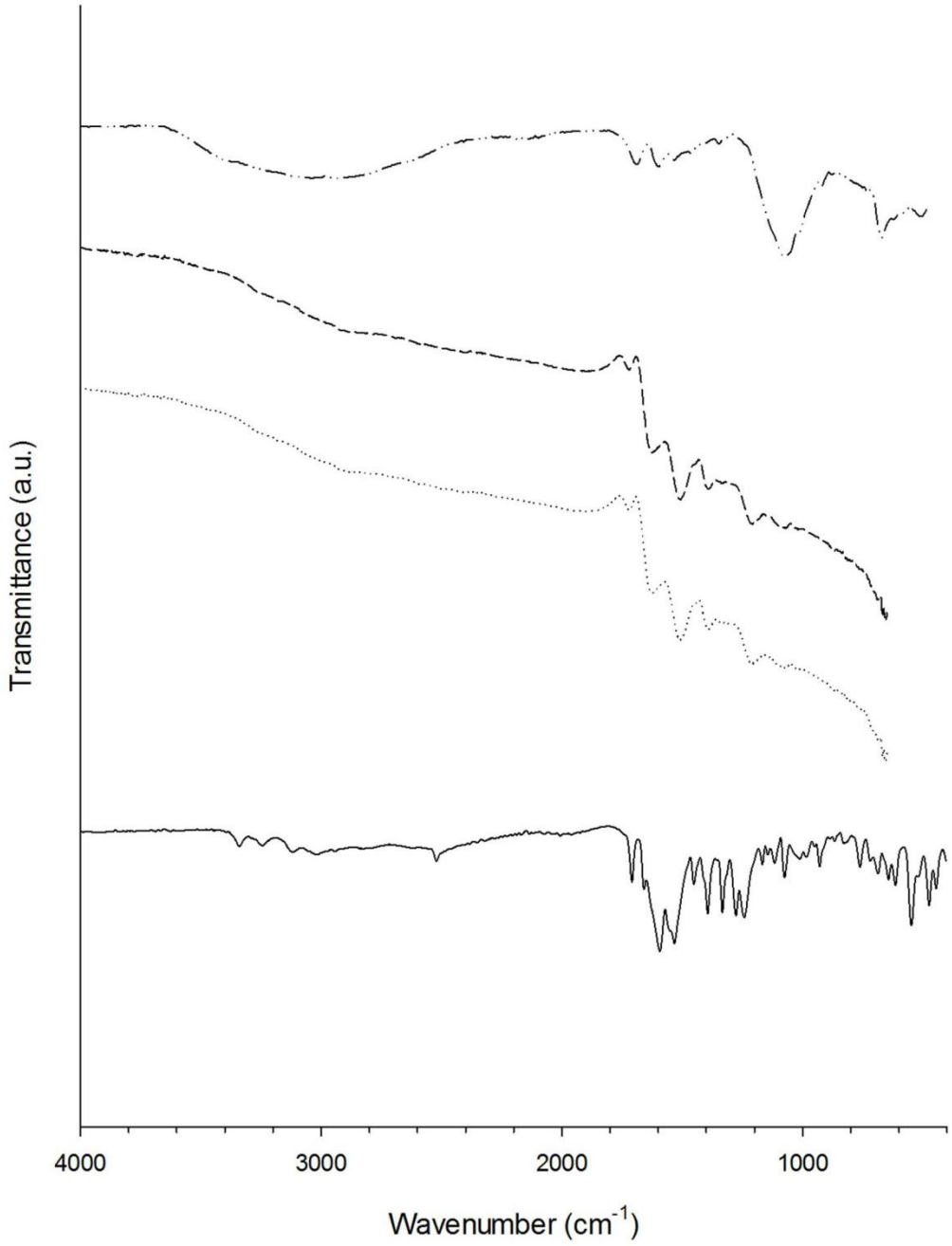

376

377 Figure 4

378

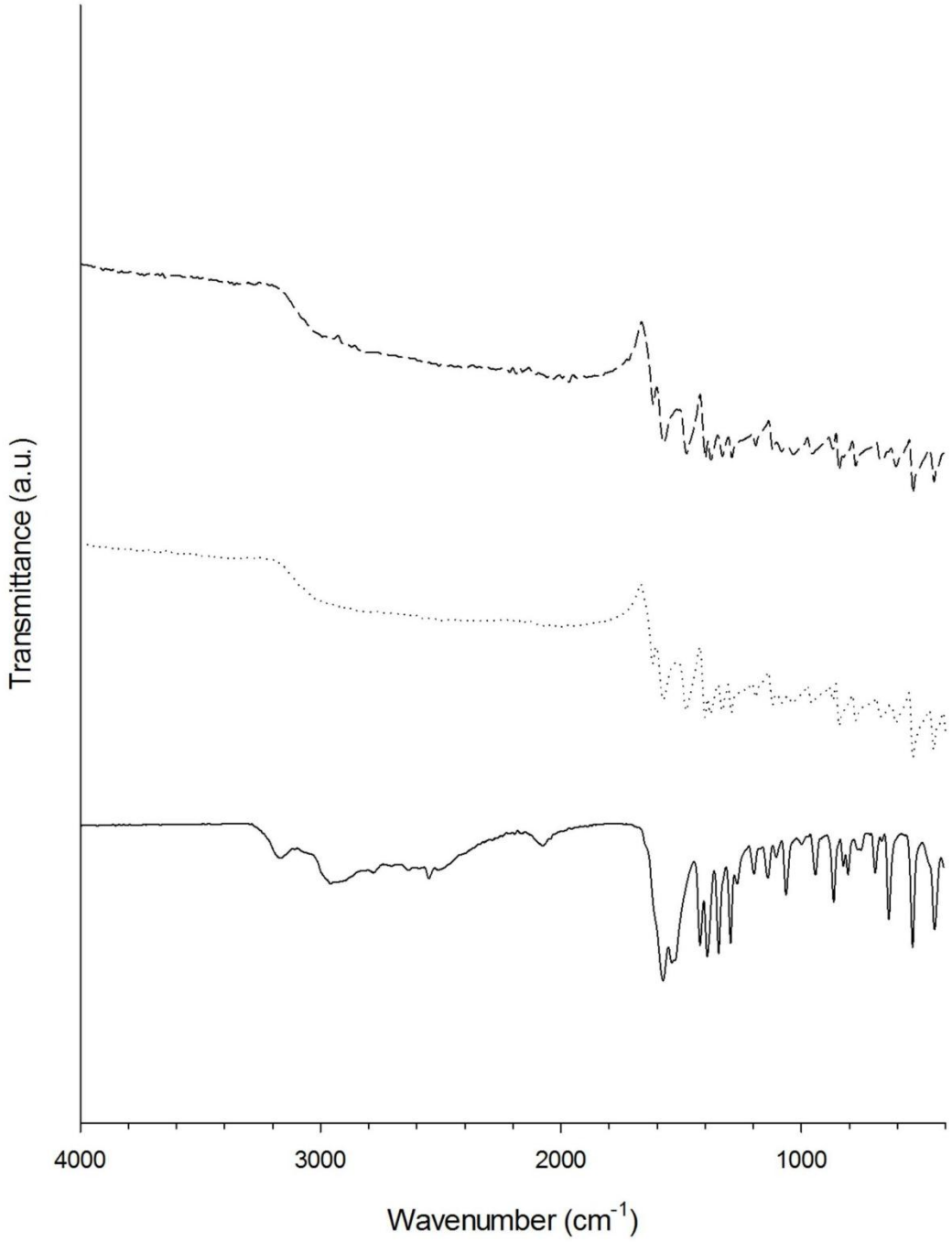

379

380 Figure 5

381

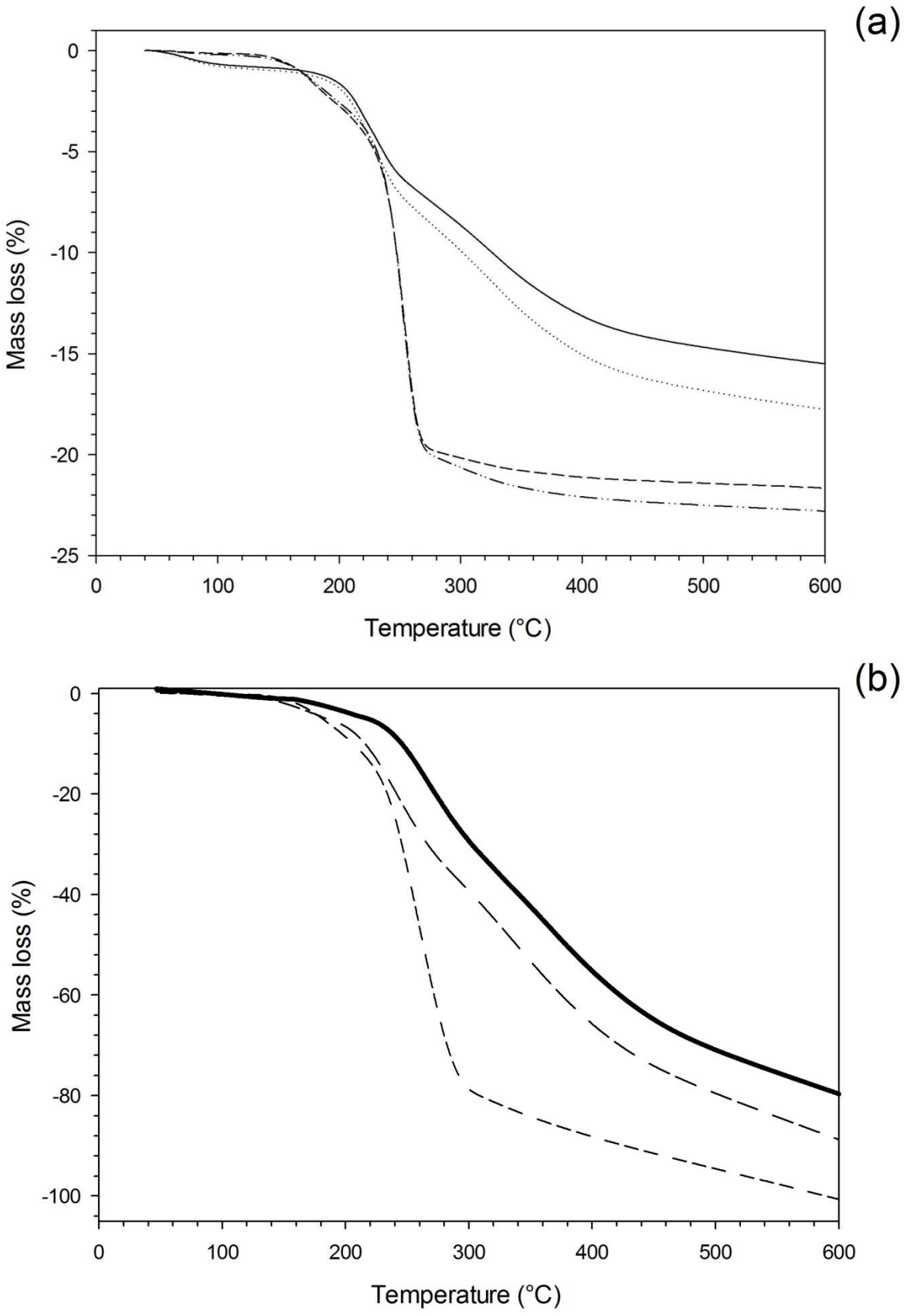

382

383 Figure 6

384

385

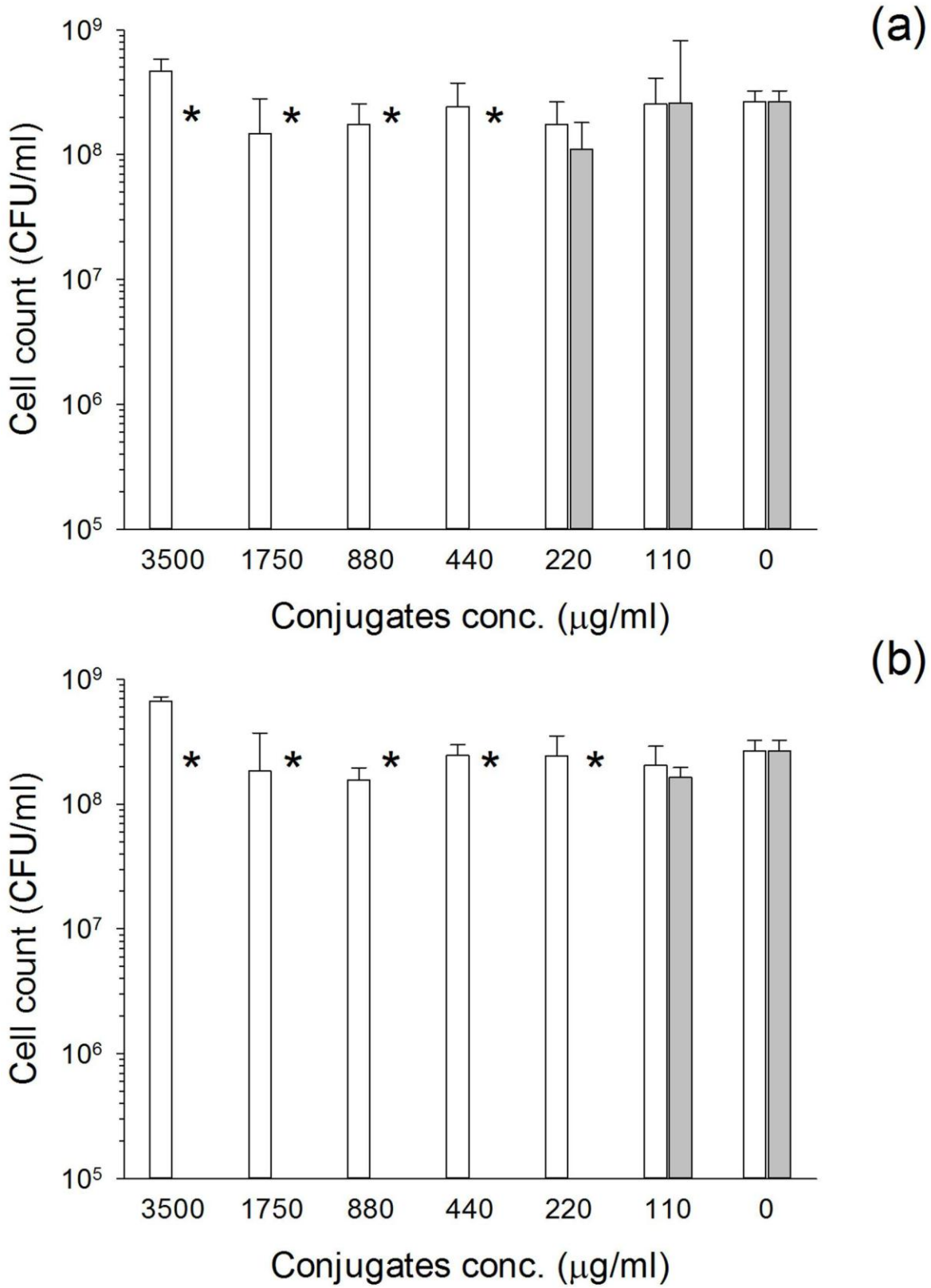

386

387 Figure 7

388

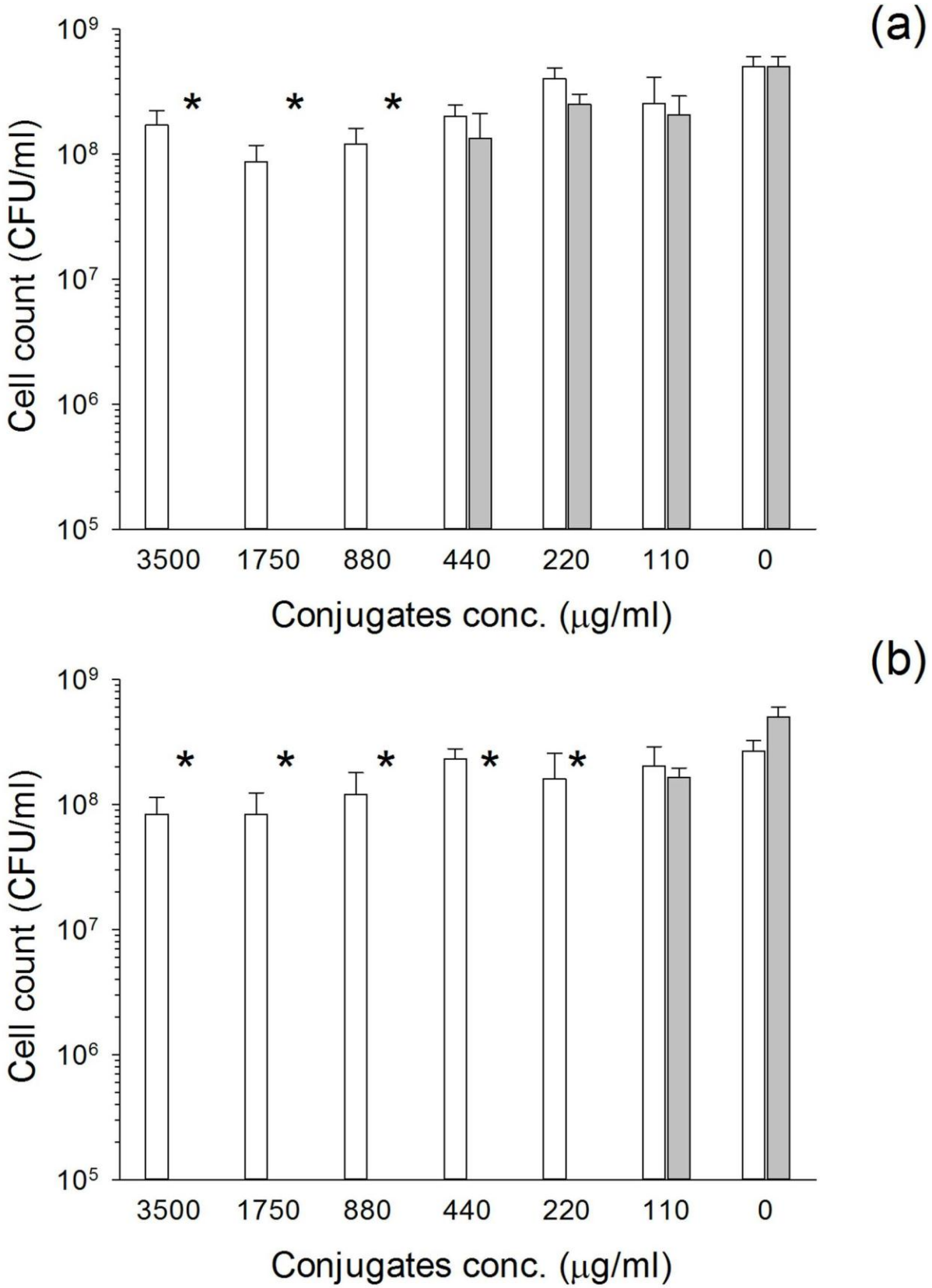

389

390 Figure 8

391

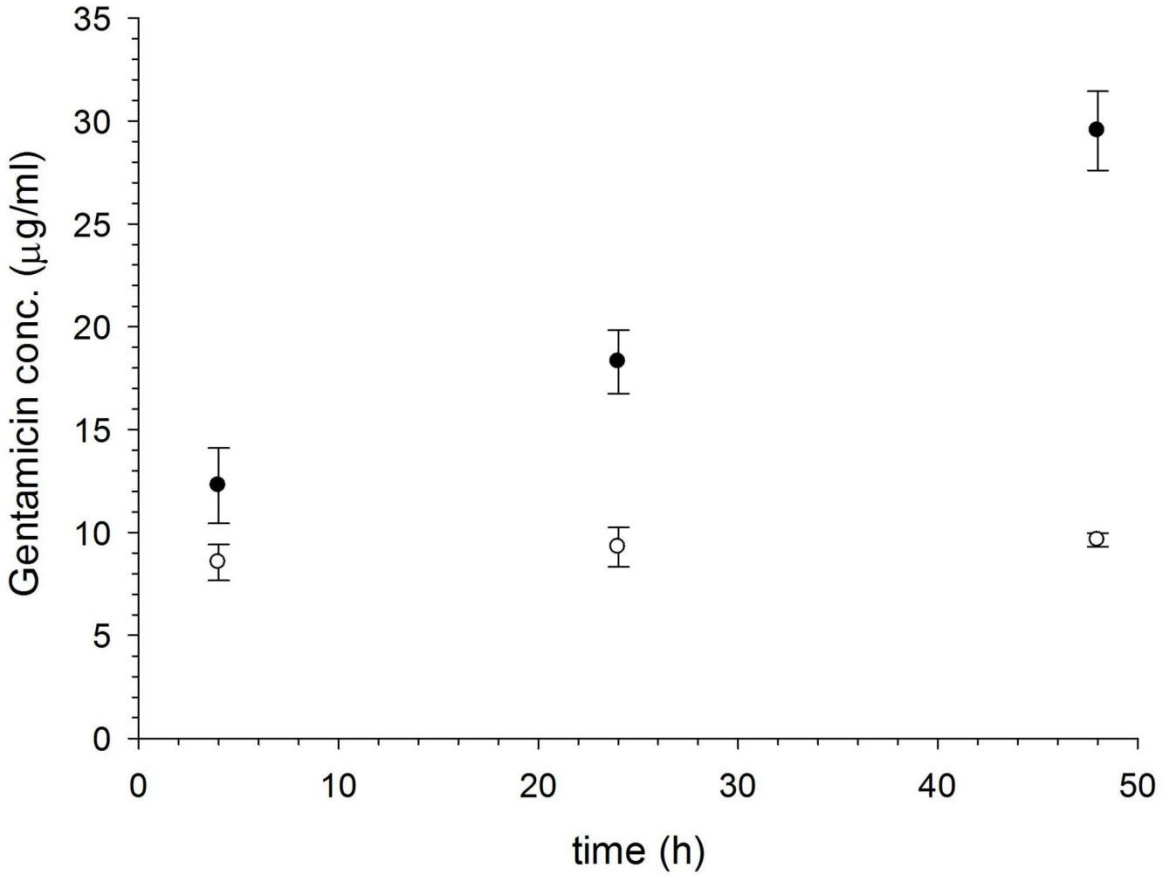

392

393 Figure 9